Dyes and Pigments 95 (2012) 221–228

Contents lists available at SciVerse ScienceDirect

Dyes and Pigments

journal homepage: www.elsevier.com/locate/dyepig

# Highly efficient soluble materials for blue phosphorescent organic light–emitting diode

Nam-Jin Lee [a], Dae-Hee Lee [a], Dong-Won Kim [a], Ji-Hoon Lee [a,**], Sang Hee Cho [b], Woo Sik Jeon [b], Jang Hyuk Kwon [b], Min Chul Suh [b,*]

[a] Department of Polymer Science & Engineering, Korea National University of Transportation, 50 Daehak-ro, Chungju-Si, Chungbuk 380-702, Republic of Korea
[b] Department of Information Display, Kyung Hee University, Dongdaemoon-Gu, Seoul 130-701, Republic of Korea

ARTICLE INFO

*Article history:*
Received 27 February 2012
Received in revised form
7 April 2012
Accepted 23 April 2012
Available online 28 April 2012

*Keywords:*
Soluble host materials
Blue phosphorescent OLED
Carbazole
Sterically bulky side groups
High triplet energy

ABSTRACT

A series of new carbazole derivatives with good solubility and electronic properties for use as host materials for blue phosphorescent organic light-emitting diodes is reported. A twisted biphenyl moiety at the center of the host materials was applied to enhance the solubility as well as triplet energies. Hence all the molecules showed good solubility as well as a fairly large triplet energy up to 3.01 eV. Blue phosphorescent devices employing bis(4,6-difluorophenylpyridinato-N,C2)picolinatoiridium (III) as the guest and the three new twisted carbazole derivatives as co-hosts with an electron type host material exhibited high efficiencies, up to 20.7 cd/A as a maximum current efficiency and 12.5% of external quantum efficiency. This performance was much improved by ~27.6%, compared to that measured for the 1,3-di(9H-carbazol-9-yl)benzene: 2,6-bis(3-(9H-carbozol-9-yl)phenyl)pyridine reference system.


## 1. Introduction

Phosphorescent organic light-emitting diodes (PHOLEDs) have attracted intense interest because of their merit of high quantum efficiency as compared to conventional fluorescent OLEDs through utilizing both singlet and triplet excitons for emission. In fact, red phosphorescent materials have already been applied in the main-display of commercial mobile phones since 2007 by Universal Display Corporation (UDC) and Samsung Mobile Display. Recently, green emission is almost approaching to the theoretical limitation of efficiency (over 20% of external quantum efficiency, EQE) by utilizing *fac*-tris(2-phenylpyridinato)iridium(III) [Ir(ppy)$_3$] as the phosphorescent emitter, and the commercialization of which is underway. Nevertheless, the development of much more efficient PHOLEDs including blue components is still required to differentiate their value from the competition with thin film transistor – liquid crystal displays (TFT-LCD) because the power consumption of TFT-LCD has been reduced significantly with the help of high performance LED backlight. However, compared with the great achievements in red and green phosphorescent materials, the blue component has many obstacles against commercialization including its short lifetime issue. Thus, many research groups concentrate on preparation of the host materials which possess: i) higher triplet energies than those of the guest molecules to realize exothermic energy transfer [1–3] to effectively confine triplet excitons within the emitting layer (EML) [4–6], ii) appropriate energy levels which can be easily aligned with those of the adjacent transporting layers for efficient charge carrier injection to result in a low driving voltage [7] and iii) moderate charge carrier mobility to increase the opportunity for electron and hole recombination within the EML [8]. For this purpose, many achievements have been reported in this field in recent years. Especially, the host materials with carbazoles [9,10], aryl silanes [11,12] and phosphine oxides [13–15] showed great progress in the device performances. Among them carbazole derivatives such as 1,3-di(9*H*-carbazol-9-yl) benzene (mCP) which is a sort of hole transport type host material with high triplet energy ($T_1$ = 2.9 eV) are still the best candidates for blue electrophosphorescent devices [16]. Meanwhile, there has been much interest in soluble OLED materials to realize a solution process such as ink-jet printing and nozzle printing because they are much more compatible with large area processing than common evaporation process. However, the greater part of materials showing high device performances (e.g. efficiency, operating

* Corresponding author. Tel.: +82 2 961 0694; fax: +82 2 968 6924.
** Corresponding author. Tel.: +82 43 841 5427; fax: +82 43 841 5420.
*E-mail addresses:* jihoonli@ut.ac.kr (J.-H. Lee), mcsuh@khu.ac.kr (M.C. Suh).

0143-7208/$ – see front matter © 2012 Elsevier Ltd. All rights reserved.
doi:10.1016/j.dyepig.2012.04.011

voltage, lifetime, etc.) are normally not suitable in solution processed OLEDs as itself due to an insufficient solubility, a high crystallization and phase separation tendency, and a glass transition temperature lower than that needed for solvent removal. To overcome those problems, many research groups have tried to use polyvinylcarbazole (PVK) mixed with 1,3-bis[(4-tert-butylphenyl)-1,3,4-oxidiazolyl]phenylene (OXD-7) as a basic bipolar host system because they give good amorphous film without any crystallization defects during processing [17–22]. As part of such efforts, the high efficiency, over 15% EQE, was recently reported from the blue PHOLEDs [19,20]. However, PVK based host system generally gives a high driving voltage plausibly due to its low hole mobility characteristics although it has a high triplet energy as well as a good film quality [23]. Thus, a development of solution based PHOLEDs with other soluble small molecular host systems with both hole and electron carrier transporting characteristics is required to overcome such problems. Nevertheless, most of blue PHOLEDs showed relatively high operating voltage greater than 6.5 V (at 1000 cd/m$^2$) until now.

In this study, we report three different types of host materials for blue PHOLEDs having twisted core structures to increase their triplet energies as well as solubility. The PHOLEDs containing those materials with 2,6-bis(3-(9*H*-carbozol-9-yl)phenyl)pyridine (26DCzPPy) showed moderate EQE up to 12.5%.

## 2. Experimental

### 2.1. Instruments

$^1$H and $^{13}$C-NMR spectra were recorded on a Bruker Avance 300 and 400 NMR spectrometer and chemical shifts were referenced to chloroform (7.26 ppm). All mass spectra were acquired on a hybrid ion-trap time-of-flight mass spectrometer (Shimadzu LCMS-IT-TOF, Kyoto, Japan) equipped with an ESI source (ESI-IT-TOFMS) in negative ion mode at a mass resolution of 10,000 full-width at half maximum (FWHM). Accurate masses were corrected by calibration using the sodium trifloroacetate clusters as internal references.

### 2.2. Synthesis of new host materials

#### 2.2.1. Synthesis of tert-butyl 3,6-dibromo-9H-carbazole-9-carboxylate (**1**)

3,6-dibromo-9*H*-carbazole (70 g, 0.22 mol) was dissolved in anhydrous THF (1 L) under nitrogen and stirred for 10 min at room temperature. Di-*tert*-butyldicarbonate (56.7 g, 0.26 mol) and 4-dimethylaminopyridine (3.2 g, 0.03 mol) were added to the reaction mixture. The mixture was stirred at room temperature for 12 h. After the reaction was finished, the mixture was washed three times with distilled water and extracted with ethyl acetate. The organic layer was separated, dried over anhydrous magnesium sulfate, and evaporated under reduced pressure to afford (**1**) as a white solid, yield 82%. $^1$H NMR (DMSO-$d_6$, 300 MHz) 8.52 (d, $J$ = 2.7 Hz, 2 H), 8.14 (d, $J$ = 7.3 Hz, 2 H), 7.71 (dd, $J$ = 8.9 Hz, 2 H), 1.69 (s, 9 H) ppm.

#### 2.2.2. Synthesis of 2-(4-tert-Butylphenyl)-4,4,5,5-tetramethyl-1,3,2-dioxaborolane (**2**)

*n*-Butyllithium (127.4 mL, 0.32 mol) was added to a solution of 1-bromo-4-*tert*-butylbenzene (47.5 g, 0.22 mol) in anhydrous THF (500 mL) at −78 °C under nitrogen atmosphere. The mixture was stirred for 30 min at the same temperature. And then, 2-isopropoxy-4,4,5,5-tetramethyl-1,3,2-dioxaborolane (50 mL, 0.25 mol) was added dropwise to the reaction mixture and stirred for 12 h at room temperature. The reaction mixture was poured into water and extracted with chloroform. The organic layer was separated, dried over anhydrous magnesium sulfate, and evaporated under reduced pressure to afford (**2**) as a white solid, yield 74%. $^1$H NMR ($CDCl_3$, 300 MHz) 7.82 (d, $J$ = 10.0 Hz, 2 H), 7.46 (d, $J$ = 8.0 Hz, 2 H), 1.37 (s, 12 H), 1.36 (s. 9 H) ppm.

#### 2.2.3. Synthesis of 3,6-bis(4-tert-butylphenyl)-9H-carbazole (**3**)

*tert*-Butyl 3,6-dibromo-9*H*-carbazole-9-carboxylate (24 g, 55 mmol), 2-(4-*tert*-butylphenyl)-4,4,5,5-tetramethyl-1,3,2-dioxaborolane (49 g, 188 mmol) dissolved in anhydrous toluene (300 mL) under nitrogen and stirred for 10 min at room temperature. Palladium(II) acetate (1.2 g, 10 mol%) and potassium carbonate (200 mL, 2 M aqueous solution) was added to the reaction mixture. The mixture was stirred at 70 °C for 16 h. The mixture was extracted with ethyl acetate (400 mL), and evaporated under reduced pressure. The crude compound was added in trifluoroacetic acid (TFA, 30 mL)/DMF (100 mL). The reaction mixture was stirred under nitrogen at 100 °C for 48 h. After the reaction was finished, the mixture was evaporated under reduced pressure to remove trifluoroacetic acid. The crude compound was added in NaOH (200 mL, 1N aqueous solution). White solid product was filtered and washed with ethyl acetate. The product (**3**) was isolated as a white solid, yield 80%. FT-IR (KBr, cm$^{-1}$) 3430, 3024, 2957, 2901, 2865, 1625, 1609, 1520, 1484, 1461, 1393, 1363, 1315, 1288, 1266, 1237, 1139, 1111, 1028, 1007, 888, 838, 813, 736, 565. $^1$H NMR (DMSO-$d_6$, 300 MHz) 11.35 (s, 1 H), 8.50 (s, 2 H), 7.71 (d, $J$ = 9 Hz, 6 H), 7.56 (m, 6 H), 1.54 (s, 18 H) ppm.

#### 2.2.4. Synthesis of 5,5′-dibromo-2,2′-dimethoxybiphenyl (**4**)

2,2′-dimethoxybiphenyl (12 g, 56 mmol) was dissolved in $CHCl_3$ (180 mL). The resulting solution was cooled down to 0 °C and bromine (6.35 mL, 123 mmol) was added. The mixture was stirred for 12 h. The reaction mixture was poured into excess water and extracted with chloroform. The organic layer was separated, dried over anhydrous magnesium sulfate, and evaporated under reduced pressure to afford (**4**) as a white solid, yield 94%. FT-IR (KBr, cm$^{-1}$) 3079, 3007, 2941, 2904, 2835, 1585, 1434, 1412, 1243, 1136, 1029, 873, 794, 614. $^1$H NMR ($CDCl_3$, 400 MHz) 7.43 (dd, $J$ = 2.5 Hz, 2 H), 7.32 (d, $J$ = 2.5 Hz, 2 H), 6.84 (d, $J$ = 8.8 Hz, 2 H), 3.75 (s, 6 H) ppm.

#### 2.2.5. Synthesis of 3,3′,5,5′-tetrabromobiphenyl (**5**)

*n*-Butyllithium (34.4 mL, 55 mmol) was added to a solution of 1,3,5-tribromobenzene (15.74 g, 50 mmol) in anhydrous THF (100 mL) at −78 °C under nitrogen atmosphere. The mixture was stirred for 1 h at the same temperature. And then, copper(II) chloride (7.39 g, 55 mmol) was added to the reaction mixture. The mixture was stirred for 12 h. After the reaction was finished, the mixture was washed three times with distilled water and extracted with ethyl acetate. The organic layer was separated, dried over magnesium sulfate, and evaporated under reduced pressure, then recrystallized from dichloromethane-acetone. The product (**5**) was isolated as a white solid, yield 90%. FT-IR (KBr, cm$^{-1}$) 3101, 3067, 1577, 1539, 1406, 1382, 1106, 1095, 1064, 847, 744, 670, 648. $^1$H NMR ($CDCl_3$, 400 MHz) 7.69 (t, $J$ = 1.7 Hz, 2 H), 7.59 (d, $J$ = 1.7, 4 H) ppm.

#### 2.2.6. Synthesis of 9,9′-(6,6′-dimethoxybiphenyl-3,3′-diyl)bis(9H-carbazole) (DMBC)

5,5'-dibromo-2,2′-dimethoxybiphenyl (1.5 g, 4.0 mmol), 9*H*-carbazole (1.42 g, 8.5 mmol), dissolved in anhydrous toluene (80 mL) under nitrogen. Sodium *tert*-butoxide (*t*-BuONa, 5.03 g, 50.8 mmol), tri-*tert*-butylphosphine ((*t*-Bu)$_3$P, 10 wt% in *n*-hexane, 1.2 mL, 0.8 mmol) and tris(dibenzylideneaceton)dipalladium(**0**) ($Pd_2(dba)_3$, 0.22 g, 5 mol%)] was added to the reaction mixture. The mixture was stirred at 120 °C for 48 h. After the reaction was finished, the mixture was washed three times with distilled water and extracted with ethyl acetate. The organic layer was separated,

dried over anhydrous magnesium sulfate, and evaporated under reduced pressure. The crude product was purified by silica gel column chromatography using *n*-hexane-THF (5:1) eluent to afford DMBC a white solid, yield 66%. $T_m$: 292 °C, FT-IR (KBr, $cm^{-1}$) 3049, 2987, 2926, 2829, 1595, 1494, 1453, 1336, 1312, 1244, 1231, 1180, 1145, 1044, 1025, 922, 818, 749, 724. $^1$H NMR ($CDCl_3$, 400 MHz) 8.14 (d, $J$ = 7.6 Hz, 4 H), 7.62 (d, $J$ = 2.7, 2 H), 7.52 (dd, $J$ = 2.7, 4 H), 7.46 (s, 2 H), 7.42 (td, $J$ = 7.1, 1.2 Hz, 4 H), 7.28 (td, $J$ = 7.9, 1.0 Hz, 4 H), 7.18 (d, $J$ = 8.7 Hz, 2 H), 3.92 (s, 6 H) ppm; $^{13}$C NMR ($CDCl_3$, 400 MHz) 155.8, 141.2, 130.8, 129.8, 12734, 127.3, 125.8, 123.2, 120.3, 119.7, 112.4, 109.9, 56.0 ppm. HRMS $[M + H]^+$: $m/z$ calcd. 545.2224; found 545.2226. Anal. calcd. for $C_{38}H_{28}N_2O_2$: C, 83.80; H, 5.18; N, 5.14 found: C, 83.83; H, 5.15; N, 5.14.

### 2.2.7. Synthesis of 9,9′-(6,6′-dimethoxybiphenyl-3,3′-diyl)bis(3,6-bis(4-tert-butylphenyl)-9H-carbazole) (B-DMBC)

5,5′-dibromo-2,2′-dimethoxybiphenyl (0.6 g, 1.6 mmol), 3,6-bis(4-tert-butylphenyl)-9*H*-carbazole (1.46 g, 3.4 mmol), dissolved in anhydrous toluene (50 mL) under nitrogen. Sodium *tert*-butoxide (2.01 g, 20.3 mmol), tri-*tert*-butylphosphine (10 wt% in *n*-hexane, 0.5 mL, 0.2 mmol) and tris(dibenzylideneaceton)dipalladium(**0**) (0.09 g, 6 mol%) was added to the reaction mixture. The mixture was stirred at 120 °C for 48 h. After the reaction was finished, the mixture was washed three times with distilled water and extracted with chloroform. The organic layer was separated, dried over anhydrous magnesium sulfate, and evaporated under reduced pressure. The crude product was purified by silica gel column chromatography using *n*-hexane-THF (4:1) eluent to afford B-DMBC a white solid, yield 58%. $T_m$: 324 °C, FT-IR (KBr, $cm^{-1}$) 3027, 2960, 2903, 2867, 1605, 1480, 1363, 1267, 1245, 1114, 1030, 883, 837, 809, 651, 604, 557. $^1$H NMR ($CDCl_3$, 400 MHz) 8.4 (d, $J$ = 1.5 Hz, 4 H), 7.71 (d $J$ = 3.0 Hz, 2 H), 7.70 (s, 4 H), 7.68 (d, $J$ = 1.8 Hz, 8 H), 7.59 (m $J$ = 2.7 Hz, 4 H), 7.55 (s, 2 H), 7.53 (d, $J$ = 8.4 Hz, 8 H), 7.24 (d, $J$ = 8.8 Hz, 2 H), 3.97 (s, 6 H), 1.40 (s, 36 H) ppm; $^{13}$C NMR ($CDCl_3$, 400 MHz) 155.9, 149.5, 141.0, 139.1, 133.3, 130.7, 129.8, 127.4, 127.2, 127.0, 125.8, 125.5, 123.9, 118.7, 56.1, 34.5, 31.5 ppm. Anal. calcd. for $C_{78}H_{76}N_2O_2$: C, 87.27; H, 7.14; N, 2.61 found: C, 87.31; H, 7.10; N, 2.58.

### 2.2.8. Synthesis of 3,3′,5,5′-tetra(9H-carbazole-yl)biphenyl (TCBP)

3,3′,5,5′-tetrabromobiphenyl (2.5 g, 5.3 mmol), 9*H*-carbazole (3.6 g, 21.4 mmol), dissolved in anhydrous toluene (60 mL) under nitrogen. Sodium *tert*-butoxide (4.13 g, 42.8 mmol), tri-*tert*-butylphosphine (10 wt% in *n*-hexane, 3.9 mL, 1.6 mmol) and tris(dibenzylideneaceton)dipalladium(**0**) (1.169 g, 25 mol%) was added to the reaction mixture. The mixture was stirred at 120 °C for 48 h. After the reaction was finished, the mixture was washed three times with distilled water and extracted with ethyl acetate. The organic layer was separated, dried over magnesium sulfate, and evaporated under reduced pressure. The crude product was purified by silica gel column chromatography using *n*-hexane-ethyl acetate (10:1) eluent to afford TCBP a white solid, yield 60%. $T_m$: 363 °C, FT-IR (KBr, cm-1) 3050, 1587, 1450, 1333, 1311, 1227, 1156, 1027, 922, 746, 772, 707, 648. $^1$H NMR ($CDCl_3$, 400 MHz) 8.16 (d, $J$ = 7.7 Hz, 8 H), 8.07 (d, $J$ = 1.9 Hz, 4 H), 7.92 (t, $J$ = 1.8 Hz, 2 H), 7.64 (d, $J$ = 8.2, 8 H), 7.48 (td, $J$ = 8.2, 1.0 Hz, 8 H), 7.35 (t, $J$ = 7.6 Hz, 8 H) ppm; $^{13}$C NMR ($CDCl_3$, 400 MHz) 142.9, 140.5, 140.4, 126.4, 125.0, 124.4, 123.8, 120.6, 120.5, 109.7 ppm. HRMS $[M + H]^+$: $m/z$ calcd. 815.3169; found 815.3161. Anal. calcd. for $C_{60}H_{38}N_4$: C, 88.43; H, 4.70; N, 6.87 found: C, 88.37; H, 4.71; N, 6.88.

### 2.3. Fabrication of PHOLEDs

Poly(3,4-ethylene dioxythiophene) (PEDOT) doped with poly(-styrenesulfonate) (PSS) (PEDOT:PSS) as a hole injection layer, 26DCzPPy as an electron transporting co-host in EML, 1,3,5-tri(*m*-pyrid-3-yl-phenyl)benzene (TmPyPB) as an electron transporting material were purchased from H. C. Starck GmbH. and Daejoo Electronic Material Co. and were used without purification. To fabricate PHOLEDs, a patterned indium-tin oxide (ITO) glass with a 150 nm thickness having an emission area of 4 $mm^2$ with a sheet resistance of 10–12 Ω/□ were used. A line pattern of ITO and an insulating layer to make active areas were formed by the photolithography process. The ITO glass substrate was cleaned by sonication in isopropyl alcohol (IPA) and then rinsed in deionized water. After a series of wet cleaning process, the ITO glass substrate was treated in a UV-ozone chamber prior to device fabrication. The PEDOT:PSS [CLEVIOSTM AI4083 (H.C. Stack)] as a hole injection layer was spin-coated on the ITO substrates and dried on a hot plate at 120 °C for 20 min to remove the solvent. The materials for the emission layer were dissolved in chlorobenzene and were spin and dried at 120 °C for 10 min. In case of mixed host, a blending ratio was fixed to 1:1. All solution process was performed in a dry nitrogen filled glove box at room temperature. After coating of EML, TmPyPB as an electron transporting layer was thermally deposited at a base pressure of $10^{-7}$ torr and then lithium fluoride (LiF) and Aluminum (Al) were deposited successively. The deposition rates of TmPyPB, LiF, and Al were 1, 0.5, and 5 ~ 10 Å/s, respectively.

The current density-voltage ($J$–$V$) and luminance-voltage ($L$–$V$) data of OLEDs were collected by Keithley 2635A and Minolta CS-100A, respectively. The area for measurement of OLED emission was 4 $mm^2$ for all the samples studied in this work. Electroluminescence (EL) spectra and CIE coordinate were measured by using a Minolta CS-1000 spectroradiometer.

Cyclic voltammetry experiments were performed using BASi (Bioanalytical Systems, Inc.) analysis equipment (C-3 standard). A platinum wire electrode and 150-nm ITO film on glass were used as counter- and working electrodes, respectively. Silver/silver ion (Ag wire in a 0.1 M $AgNO_3$ solution) was used as a reference electrode. The $Ag/Ag^+$ ($AgNO_3$) reference electrode was calibrated at the beginning of the experiments by running cyclic voltammetry on ferrocene as the internal standard. By means of the internal ferrocenium/ferrocene ($Fc^+$/Fc) standard, the potential values were converted to the saturated calomel electrode scale. Experiments were run on the film states of the materials that were used. The films that had been coated with these materials were made on ITO glass through the solution drop coating. A 0.1 M $Bu_4NClO_4$ (tetrabutylammonium perchlorate) electrolyte solution in acetonitrile was used in all the experiments.

## 3. Results and discussion

### 3.1. Materials

Three host materials were prepared to realize a highly efficient blue PHOLED. Carbazole moieties were selected as a key functionality because they have proved to afford immensely successful results as blue PHOLEDs when utilized with bis(4,6-difluorophenylpyridinato-N,C2)picolinatoiridium (III) (FIrpic) [24]. In principle, carbazole containing host materials exhibit high triplet energies if they have no extended π-conjugation length [25,26]. In other words, the most common approach to increase a triplet energy level as a blue host might be the disruption of π-conjugation just as in the case of mCP which has two carbazole units connected by the meta position of a single benzene ring and shows high triplet energy level up to 2.9 eV. Thus, we used the mCP units as a main functional moiety and connected to the biphenyl core structure with sterically hindered methoxy groups in the 6,6′-position, which result in steric crowding such as in 4,4′-Bis-(9-carbazolyl)-biphenyl (CBP) derivatives with methyl or trifluoromethyl groups in the 2,2′-

position of the biphenyl group which are prepared by Schrögel et al. [25]. This approach gives higher molecular weight species which could be associated with an improved thermal stability of the host materials for blue PHOLED. In addition, a new host material simply having sterically hindered four carbazole moieties in its 3,3′,5,5′-position was also prepared as shown in Scheme 1. Fig. 1 shows the geometries of core parts of those three resultant host materials obtained from the simulation at a DNP/GGA(PBE) level of theory using Dmol3 module (Material Studio, Accelrys software). The biphenyl moieties were significantly twisted which results in diminished conjugation as we expected. This approach could also be helpful to improve the solubility of the materials because these materials do not tend to stack due to a larger vacant volume which results from the steric distortions.

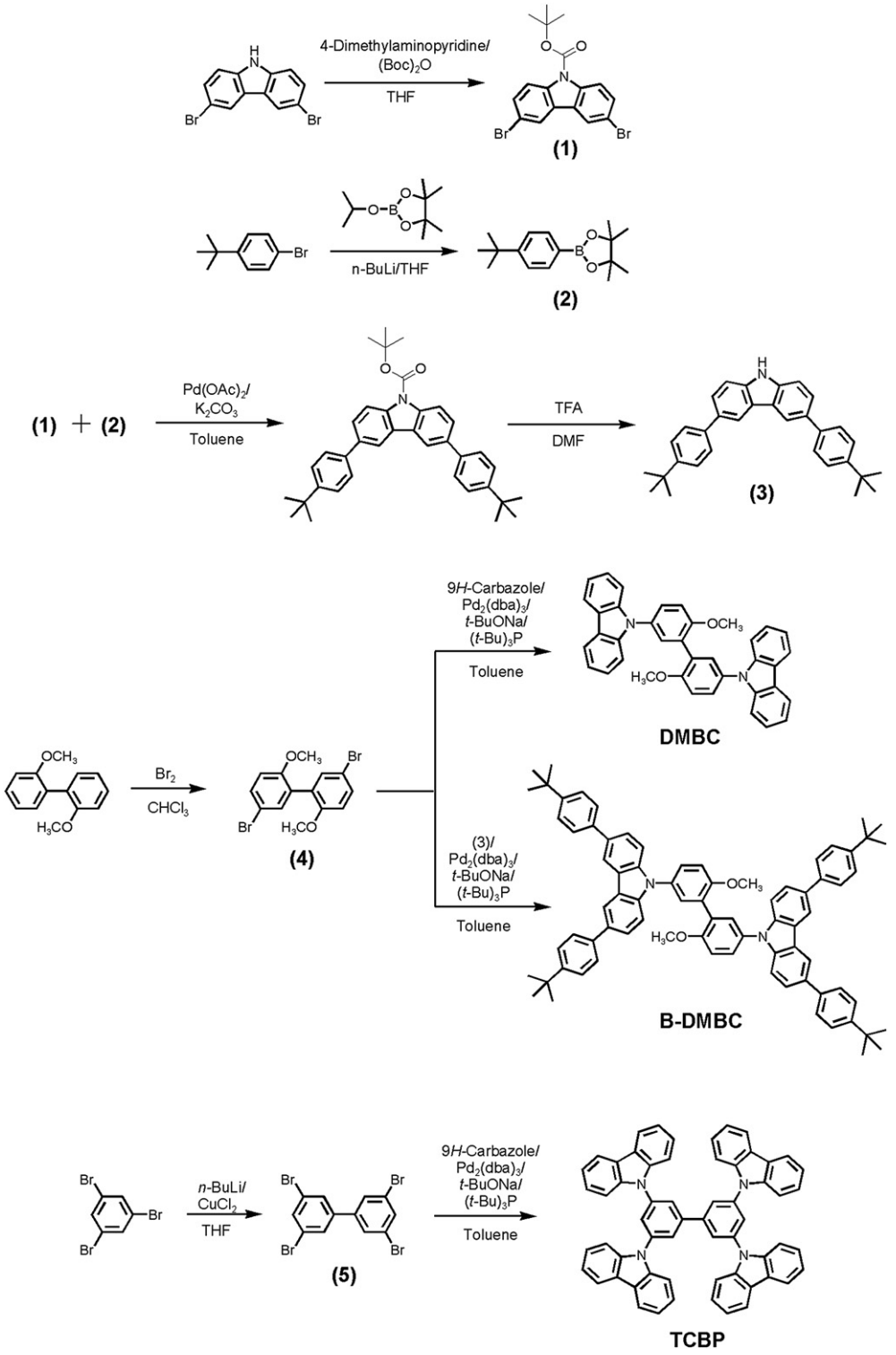


**Scheme 1.** Synthesis of carbazole derivatives for blue PHOLEDs.

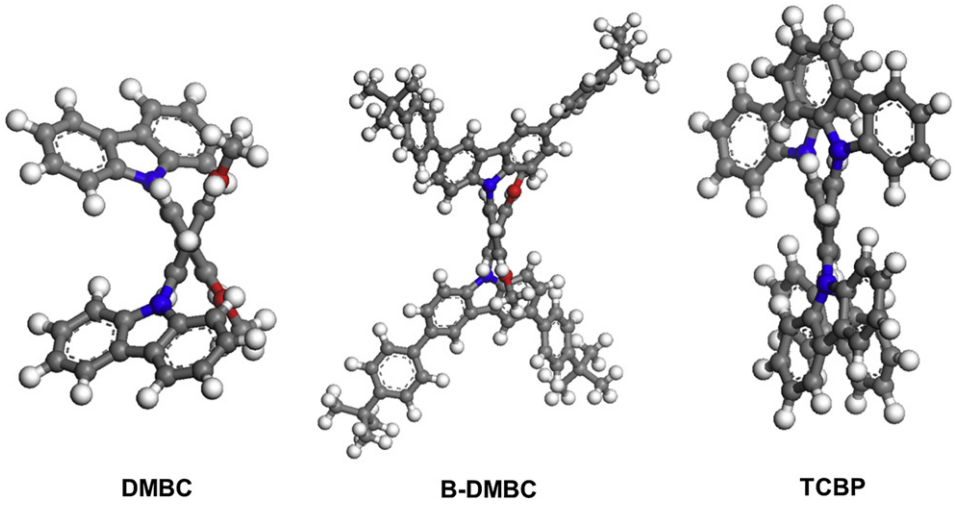


**Fig. 1.** Geometries of three host materials having twisted core structures.

Fig. 2 shows the UV–vis absorption and photoluminescence spectra of new host materials in 2-methyl tetrahydrofuran. **DMBC** and **TCBP** showed similar absorption behavior, in which the two lower-lying bands that appear in the region of ~ 320–335 and 335–350 nm which are tentatively assigned to the $n \rightarrow \pi^*$ transitions as shown Fig. 2(a). Very interestingly, **TCBP** showed a slightly larger band gap (3.57 eV) than **DMBC** molecule (3.49 eV) presumably due to a serious disruption of π-conjugation from the much more hindered stereo-interaction among carbazole moieties. On the contrary to those materials, **B-DMBC** showed much smaller band gap (~3.30 eV) due to its extended conjugation length presumably due to its relatively less twisted core geometry as shown in Fig. 1. All three compounds showed vibronic fine structures in their emission spectra, especially at the low temperature (77 K) as shown in Fig. 2(b). The triplet energies (T1) of new host materials which were determined from the phosphorescence peak wavelength of the low temperature PL spectra were 3.02, 2.75, 2.79 eV for **DMBC**, **B-DMBC**, and **TCBP** respectively as shown in Fig. 2(b) and the representative results are summarized in Table 1. The energy levels of Highest Occupied Molecular Orbital (HOMO) and Lowest Unoccupied Molecular Orbital (LUMO) were collected from cyclic voltammetry and band edges of UV–vis absorption spectra and they were also summarized in Table 1.

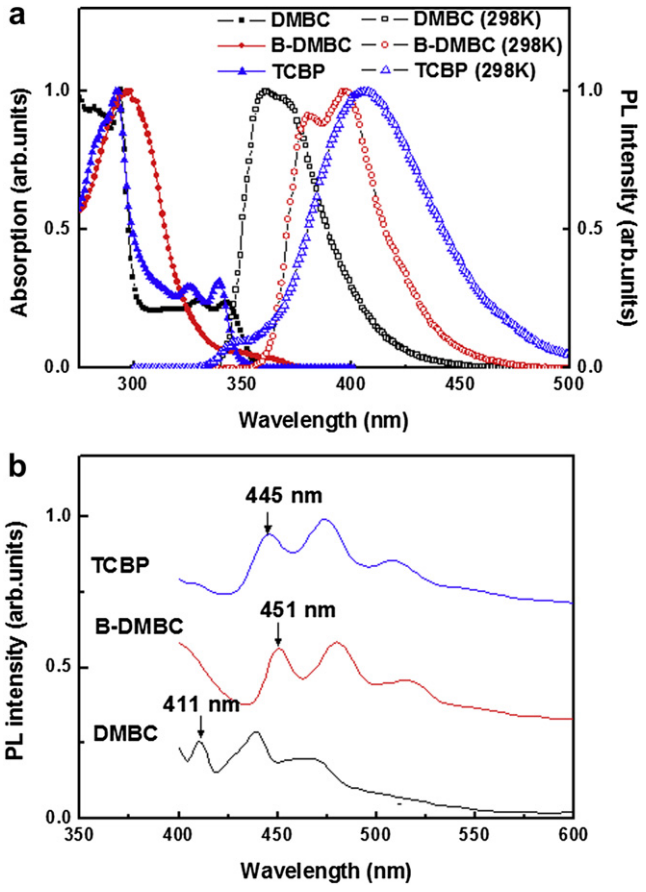


**Fig. 2.** (a) UV–visible absorption and photoluminescence spectra (at 298 K), (b) photoluminescence spectra (at 77 K) of three host materials in 2-methyl tetrahydrofuran.

Besides, the molecular orbitals of **DMBC**, **B-DMBC**, and **TCBP** are shown in Fig. 3. As we expected from the molecular structure, the electrons in HOMO was localized on the carbazole unit, while the electrons in LUMO was dispersed over the biphenyl core unit.

### 3.2. Device characteristics

The chemical structures of newly synthesized host materials and other materials for blue PHOLEDs in this study are shown in Fig. 4.

For the remarkable enhancement of efficiency upon doping, the bipolar character of host materials with an appropriate triplet energy level is very important. To satisfy this requirement, we utilized 1:1 mixed host system of those new host materials with 26DCzPPy having relatively high electron transporting property as well as high triplet energy [electron mobility ($\mu_e$) of 26DCzPPy : $2 \times 10^{-5}$ $cm^2$ $V^{-1}s^{-1}$; $T_1 = 2.71$ eV] [27]. In addition, we selected TmPyPB as an electron transport layer (ETL) due to its high triplet

**Table 1**
Summary of physical properties of new host materials.

| | Absorption (nm) | △ Eg (eV) | PL (nm) | T1 (eV) | HOMO | LUMO |
|---|---|---|---|---|---|---|
| DMBC | 293, 629, 343 | 3.49 (355 nm) | 360 | 3.02 (411 nm) | 5.61 | 2.12 |
| B-DMBC | 297, 346, 362 | 3.30 (375 nm) | 380, 397 | 2.75 (451 nm) | 5.51 | 2.21 |
| TCBP | 293, 325, 339 | 3.57 (347 nm) | 406 | 2.79 (445 nm) | 5.69 | 2.12 |

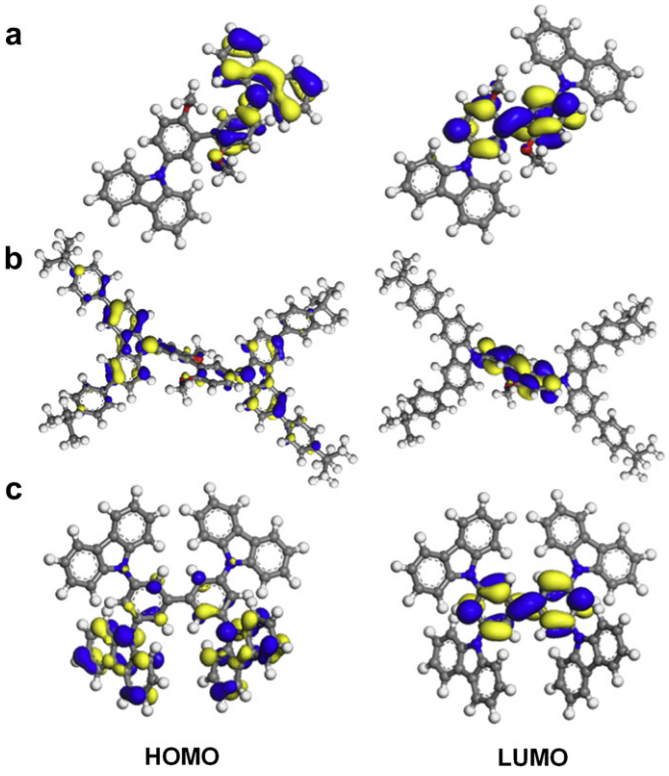


**Fig. 3.** HOMO and LUMO shapes of three host materials.

energy ($T_1 = 2.7$ eV) which gives a favorable energy transfer inside EML without exciton quenching at the neighboring non-emissive layers. The device structures tested in this study are shown in Fig. 5. The exact device configuration used in this work was as follows:

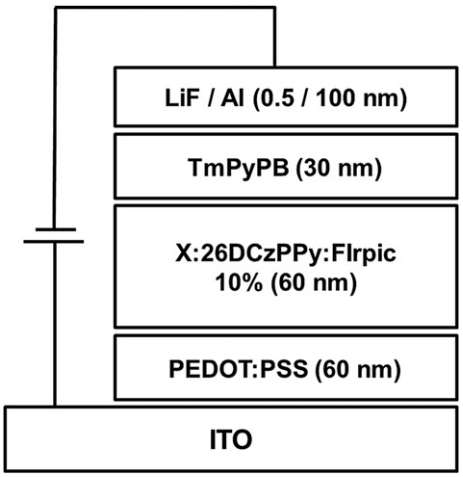


**Fig. 5.** Schematic diagram of device architecture of blue PHOLEDs fabricated in this study.

**Device A**: ITO/PEDOT:PSS (60 nm)/mCP:26DCzPPy:FIrpic (10%, 60 nm)/TmPyPB (30 nm)/LiF (0.5 nm)/Al (100 nm)
**Device B**: ITO/PEDOT:PSS (60 nm)/**DMBC**:26DCzPPy:FIrpic (10%, 60 nm)/TmPyPB (30 nm)/LiF (0.5 nm)/Al (100 nm)
**Device C**: ITO/PEDOT:PSS (60 nm)/**B-DMBC**:26DCzPPy:FIrpic (10%, 60 nm)/TmPyPB (30 nm)/LiF (0.5 nm)/Al (100 nm)
**Device D**: ITO/PEDOT:PSS (60 nm)/**TCBP**:26DCzPPy:FIrpic (10%, 60 nm)/TmPyPB (30 nm)/LiF (0.5 nm)/Al (100 nm)

Fig. 6(a) shows the $J$–$V$ and $L$–$V$ characteristics of fabricated blue PHOLEDs and the representative results are summarized in Table 2. At a given constant voltage of 7.0 V, current density values of 5.3, 8.9, 5.8, and 4.8 mA/cm$^2$ were observed in the fabricated PHOLEDs A, B, C, and D, respectively. The driving voltages to reach 1000 cd/m$^2$ were 7.0, 6.6, 7.4, and 8.6 V for the PHOLEDs A, B, C, and

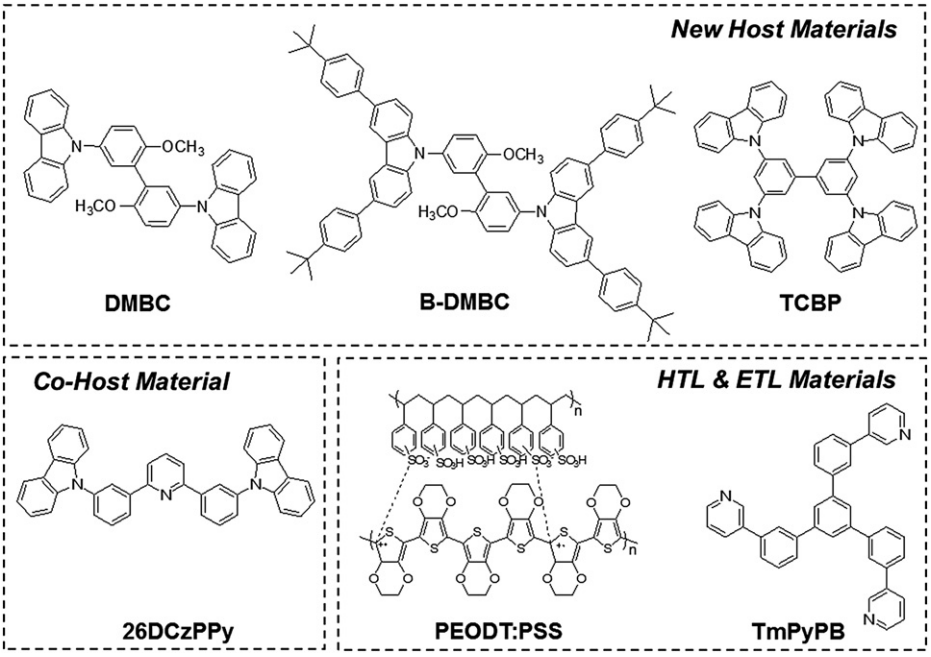


**Fig. 4.** Chemical structures of the materials for blue PHOLEDs fabricated in this study. (For interpretation of the references to colour in this figure legend, the reader is referred to the web version of this article.)

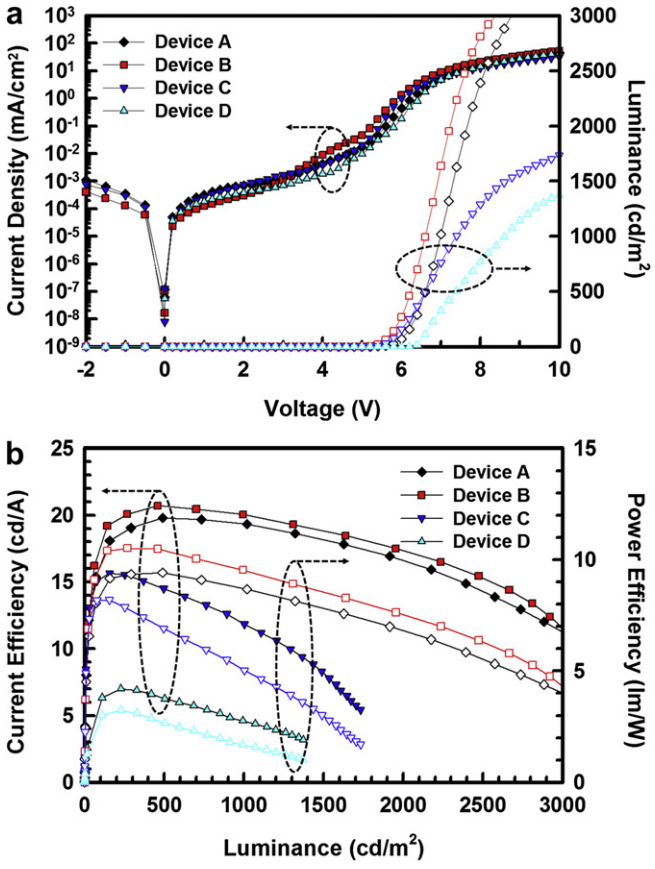


**Fig. 6.** a) $J-V-L$ characteristics of fabricated blue PHOLEDs. b) Luminance vs current efficiency and power efficiency characteristics of fabricated blue PHOLEDs. (For interpretation of the references to colour in this figure legend, the reader is referred to the web version of this article.)

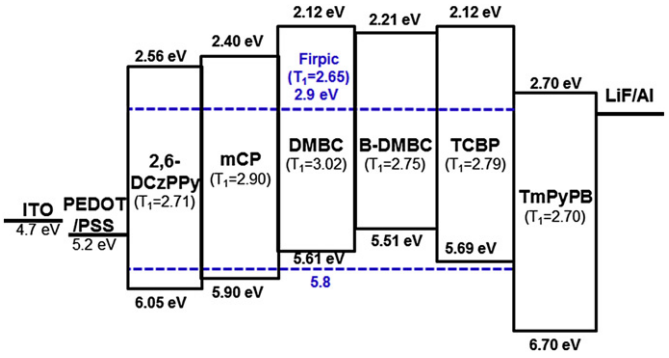


**Fig. 7.** Energy band diagrams of used materials in this work.

D, respectively (Table 2). The relatively high turn-on voltages of 5.4, 5.0, 5.2, and 6.2 V were observed for the PHOLEDs A, B, C, and D, respectively. In the described PHOLED configuration, relatively high driving voltage performances might be attributed to the relatively high energy barrier in between PEDOT/PSS and the new synthetic host materials as shown in Fig. 7. Meanwhile, the PHOLED B with **DMBC** showed the greatest current density at the observed driving voltage region and the operating voltage at 1000 cd/m$^2$ of brightness was observed to be ~6.6 V which is the lowest among the devices fabricated in this study presumably due to a relatively higher lying HOMO level (~5.61 eV) of **DMBC** (cf. PHOLED A with mCP: 7.0 V at 1000 cd/m$^2$, HOMO: 5.90 eV). However, the PHOLED C with **B-DMBC** which is a very bulky molecule and was prepared as a highly soluble host material in common organic solvents, showed a relatively high operating voltage of ~7.4 V. From the density functional theory (DFT) calculations, the LUMOs in **DMBC**, **B-DMBC**, and **TCBP** are more concentrated on the center of the molecules and the electron hopping distances are dependent upon the sizes of the neighboring substituents as shown in Fig. 3. On the other hand, the HOMO in **DMBC**, **B-DMBC**, and **TCBP** are localized on the carbazoles at the ends of the molecules (See also Fig. 3). Thus, 4-tert-butylphenyl moieties which are utilized as solubilizing groups in **B-DMBC** molecule may increase the hopping distances in between HOMOs or LUMOs compared to those in **DMBC** molecule. Thus, the charge-transfer integral of **B-DMBC** might be smaller than that of **DMBC** which causes an increased operating voltage [28]. Similarly, the HOMOs in **TCBP** are localized in four neighboring carbazole moieties. However, those moieties may disturb the molecular stacking due to a totally distorted steric interaction between the four carbazole units around the biphenyl moiety which causes a disturbed charge carrier hopping process (through p-orbital interaction). Hence the operating voltage of PHOLED D with **TCBP** was even higher (~8.6 V) than that from the PHOLED C with **B-DMBC**.

The current and power efficiency characteristics of the fabricated PHOLEDs are shown in Fig. 6(b) and also summarized in Table 2. At a given constant luminance of 1000 cd/m$^2$, the current and power efficiencies were 19.3 cd/A and 8.7 lm/W for the PHOLED A, 20.0 cd/A and 9.5 lm/W for the PHOLED B, 11.8 cd/A and 5.0 lm/W for the PHOLED C, 4.6 cd/A and 1.7 lm/W for the PHOLED D, respectively. These efficiency data correspond to 9.8, 12.5, 5.3, and 2.0% external quantum efficiencies of PHOLEDs A, B, C and D, respectively. The maximum current and power efficiencies were 19.8 cd/A and 9.4 lm/W for the PHOLED A, 20.7 cd/A and 10.5 lm/W for the PHOLED B, 15.7 cd/A and 8.2 lm/W for the PHOLED C, 7.0 cd/A and 3.0 lm/W for the PHOLED D, respectively.

Fig. 8 shows the EL spectra at a brightness of 1000 cd/m$^2$ of different fabricated blue PHOLEDs. The PHOLEDs A, B, C showed similar EL spectra. However, PHOLED D with **TCBP** showed a significant red shift in the EL spectra, that is, the color coordinate was changed from (0.17, 0.28) to (0.18, 0.31). From this phenomena, we could presume that the recombination zone of PHOLED A, B, C with mCP:26DCzPPy:FIrpic, **DMBC**:26DCzPPy:FIrpic, **B-DMBC**:26DCzPPy:FIrpic systems are approximately in the center through ETL side of EML due to preferred charge (hole) carrier

**Table 2**
Device characteristics of phosphorescent blue OLEDs.

| | Device A | Device B | Device C | Device D |
|---|---|---|---|---|
| Turn-on voltage (1 cd/m$^2$) | 5.4 V | 5.0 V | 5.2 V | 6.2 V |
| Operating voltage (1000 cd/m$^2$) | 7.0 V | 6.6 V | 7.4 V | 8.6 V |
| Efficiency (1000 cd/m$^2$) | 19.3 cd/A 8.7 lm/W | 20.0 cd/A 9.5 lm/W | 11.8 cd/A 5.0 lm/W | 4.6 cd/A 1.7 lm/W |
| Efficiency (Max) | 19.8 cd/A 9.4 lm/W | 20.7 cd/A 10.5 lm/W | 15.7 cd/A 8.2 lm/W | 7.0 cd/A 3.0 lm/W |
| CIE (x,y) (1000 cd/m$^2$) | 0.169, 0.284 | 0.167, 0.278 | 0.169, 0.288 | 0.184, 0.313 |
| E.Q.E. (1000 cd/m$^2$) | 9.8% | 12.5% | 5.3% | 2.0% |

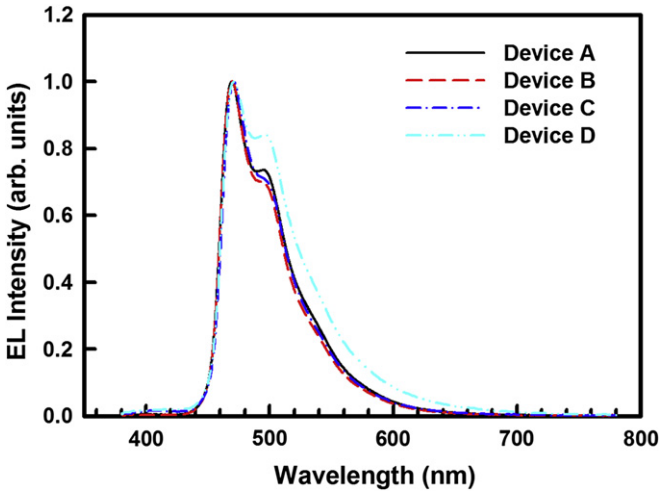


**Fig. 8.** EL spectra at a brightness of 1000 cd/m$^2$ of different fabricated blue PHOLEDs. (For interpretation of the references to colour in this figure legend, the reader is referred to the web version of this article.)

mobility of those materials. However, it would be shifted to the hole transport layer (HTL)/EML interface in case of PHOLED D with **TCBP**:26DCzPPy:FIrpic presumably due to a decreased hole conductivity due to a lower order of molecular stacking order. However, this is not desirable because the excitons generated in this interface could be quenched by the PEDOT:PSS layer. Hence, we observed very low efficiency (~2%) when we use a **TCBP** as a co-host material of PHOLED in this study. In other words, balanced exciton recombination in the EML could be achieved when we use a mCP, **DMBC**, **B-DMBC** as co-host materials with 26DCzPPy and **DMBC** is the most desirable material for the blue PHOLED fabrication.

## 4. Conclusion

In conclusion, we report new soluble host materials with sterically bulky side groups which are bonded to a significantly twisted biphenyl core unit to realize a highly efficient blue PHOLED. Every host materials having carbazole moieties showed improved hole transporting properties as well as the enhanced triplet energy up to 3.02 eV by breaking the conjugation length of the host materials. The PHOLEDs prepared by these host materials with soluble PEDOT:PSS showed moderately efficient and bright blue phosphorescence emission with EQE (External Quantum Efficiency) of ~12.5% in case of host with **DMBC** molecule.

## Acknowledgments

Prof. J.-H. Lee acknowledges to Basic Science Research Program through the National Research Foundation of Korea (NRF) funded by the Ministry of Education, Science and Technology (Grant No. NRF-2010-0012463). Prof. M. C. Suh gratefully acknowledges to Basic Science Research Program through the National Research Foundation of Korea (NRF) funded by the Ministry of Education, Science and Technology (Grant No. NRF-2011-0006847). High resolution mass spectroscopy was carried out at Korea Basic Science Institute (Mass Spectrometry Research Team).

## References

[1] Holmes RJ, Forrest SR, Tung YJ, Kwong RC, Brown JJ, Garon S, et al. Blue organic electrophosphorescence using exothermic host–guest energy transfer. Applied Physics Letters 2003;82:2422–4.
[2] Kawamura Y, Goushi K, Brooks J, Brown JJ, Sasabe H, Adachi C. 100% phosphorescence quantum efficiency of Ir(III) complexes in organic semiconductor films. Applied Physics Letters 2005;86:071104.
[3] Tokito S, Iijima T, Suzuri Y, Kita H, Tsuzuki T, Sato F. Confinement of triplet energy on phosphorescent molecules for highly-efficient organic blue-light-emitting devices. Applied Physics Letters 2003;83:569–71.
[4] Goushi K, Kwong R, Brown JJ, Sasabe H, Adachi C. Triplet exciton confinement and unconfinement by adjacent hole-transport layers. Journal of Applied Physics Letters 2004;95:7798–802.
[5] Lee J, Chopra N, Eom SH, Zheng Y, Xue J, So F, et al. Effects of triplet energies and transporting properties of carrier transporting materials on blue phosphorescent organic light emitting devices. Applied Physics Letters 2008;93:123306.
[6] Jeon WS, Kulshreshtha C, Yu JH, Lim MJ, Park JS, Kwon JH. High efficiency green phosphorescent OLEDs with triplet exciton confinement architecture. Current Applied Physics 2011;11:311–4.
[7] Kim SY, Jeon WS, Park TJ, Pode R, Jang J, Kwon JH. Low voltage efficient simple p-i-n type electrophosphorescent green organic light-emitting devices. Applied Physics Letters 2009;94:133303.
[8] Su SJ, Chiba T, Takeda T, Kido J. Pyridine-containing triphenylbenzene derivatives with high electron mobility for highly efficient phosphorescent OLEDs. Advanced Materials 2008;20:2125–30.
[9] Tsai MH, Hong YH, Chang CH, Su HC, Wu CC, Matoliukstyte A, et al. 3-(9-carbazolyl)carbazoles and 3,6-Di(9-carbazolyl)carbazoles as effective host materials for efficient blue organic electrophosphorescence. Advanced Materials 2007;19:862–6.
[10] Sasabe H, Pu YJ, Nakayama K, Kido J. m-Terphenyl-modified carbazole host material for highly efficient blue and green PHOLEDS. Chemical Communications 2009:6655–7.
[11] Holmes RJ, D'Andrade BW, Forrest SR, Ren X, Li J, Thompson ME. Efficient, deep-blue organic electrophosphorescence by guest charge trapping. Applied Physics Letters 2003;83:3818–20.
[12] Ren X, Li J, Holmes RJ, Djurovich PI, Forrest SR, Thompson ME. Ultrahigh energy gap hosts in deep blue organic electrophosphorescent devices. Chemitry of Materials 2004;16:4743–7.
[13] Lee J, Lee JI, Lee JY, Chu HY. Improved performance of blue phosphorescent organic light-emitting diodes with a mixed host system. Applied Physics Letters 2009;95:253304–13.
[14] Chou HH, Cheng CH. A highly efficient universal bipolar host for blue, green, and red phosphorescent OLEDs. Advanced Materials 2010;22:2468–71.
[15] Jeon SO, Yook KS, Joo CW, Lee JY. High-efficiency deep-blue-phosphorescent organic light-emitting diodes using a phosphine oxide and a phosphine sulfide high-triplet-energy host material with bipolar charge-transport properties. Advanced Materials 2010;22:1872–6.
[16] Lee JH, Lee JI, Song KI, Lee SJ, Chu HY. Influence of doping profile on the efficiency of blue phosphorescent organic light-emitting diodes. Applied Physics Letters 2008;92:133304.
[17] Hou L, Duan L, Qiao J, Li W, Zhang D, Qiu Y. Efficient single layer solution-processed blue-emitting electrophosphorescent devices based on a small-molecule host. Applied Physics Letters 2008;92:263301.
[18] Ye S, Liu Y, Chen J, Lu K, Wu W, Du C, et al. Solution-processed solid solution of a novel carbazole derivative for high-performance blue phosphorescent organic light-emitting diodes. Advanced Materials 2010;22:4167–71.
[19] Jiang W, Duan L, Qiao J, Zhang D, Dong G, Wang L, et al. Novel star-shaped host materials for highly efficient solution-processed phosphorescent organic light-emitting diodes. Journal of Materials Chemistry 2010;20:6131–7.
[20] Earmme T, Ahmed E, Jenekhe SA. Solution-processed highly efficient blue phosphorescent polymer light-emitting diodes enabled by a new electron transport material. Advanced Materials 2010;22:4744–8.
[21] Mathai MK, Choong V, Choulis SA, Krummacher B, So F. Highly efficient solution processed blue organic electrophosphorescence with 14lm/W luminous efficacy. Applied Physics Letters 2006;88:243512–3.
[22] Huang F, Shih PI, Liu MS, Shu CF, Jen AKY. Lithium salt doped conjugated polymers as electron transporting materials for highly efficient blue polymer light-emitting diodes. Applied Physics Letters 2008;93:243302–3.
[23] Xiao L, Chen Z, Qu B, Luo J, Kong S, Gong Q, et al. Recent progresses on materials for electrophosphorescent organic light-emitting devices. Advanced Materials 2011;23:926–52.
[24] Tsai MH, Lin HW, Su HC, Ke TH, Wu CC, Fang FC, et al. Highly efficient organic blue electrophosphorescent devices based on 3,6-bis(triphenylsilyl)carbazole as the host material. Advanced Materials 2006;18:1216–20.
[25] Schrögel P, Tomkevičienė A, Strohriegl P, Hoffmann ST, Köhler A, Lennartz C. A series of CBP-derivatives as host materials for blue phosphorescent organic light-emitting diodes. Journal of Materials Chemistry 2011;21:2266–73.
[26] Gong S, He X, Chen Y, Jiang Z, Zhong C, Ma D, et al. Simple CBP isomers with high triplet energies for highly efficient blue electrophosphorescence. Journal of Materials Chemistry 2012;22:2894–9.
[27] Cai C, Su SJ, Chiba T, Sasabe H, Pu YJ, Nakayama K, et al. High-efficiency red, green and blue phosphorescent homojunction organic light-emitting diodes based on bipolar host materials. Organic Electronics 2011;12:843–50.
[28] Tse SC, So SK, Yeung MY, Lo CF, Wen SW, Chen CH. The role of charge-transfer integral in determining and engineering the carrier mobilities of 9,10-di(2-naphthyl)anthracene compounds. Chemical Physics Letters 2006;422:354–7.